Molecular Pharmacology Fast Forward. Published on January 12, 2015 as DOI: 10.1124/mol.114.096701
This article has not been copyedited and formatted. The final version may differ from this version.

Rapid Throughput Analysis Demonstrates that Chemicals with Distinct Seizurogenic Mechanisms Differentially Alter Ca^{2+} Dynamics in Networks Formed by Hippocampal Neurons in Culture

Zhengyu Cao, Xiaohan Zou, Yanjun Cui, Susan Hulsizer, Pamela J. Lein, Heike Wulff, and Isaac N. Pessah

State Key Laboratory of Natural Medicines and Jiangsu Provincial Key laboratory for TCM Evaluation and Translational Development, China Pharmaceutical University, Nanjing, P.R. China, 211198 (Z.C., X.Z., Y.C.); Department of Molecular Biosciences, School of Veterinary Medicine, University of California, Davis, 95616 (Z.C., Y.C., S.H., P.J.L., I.N.P.); and Department of Pharmacology, School of Medicine, University of California, Davis, 95616 (H.W.)

Molecular Pharmacology Fast Forward. Published on January 12, 2015 as DOI: 10.1124/mol.114.096701
This article has not been copyedited and formatted. The final version may differ from this version.

Running Title: Rapid-throughput SCO Analysis of Seizurogenic Agents

Corresponding author:

Isaac N. Pessah

Department of Molecular Biosciences,

School of Veterinary Medicine

1089 Veterinary Medicine Drive

University of California, Davis

One Shields Avenue, Davis, CA 95616

E-mail: inpessah@ucdavis.edu

Tel: 530-752-6696

FAX: 530-752-4698

Number of:

Text Pages (29)

Tables (0)

Figures (9)

References (59)

Number of words:

Abstract (249)

Introduction (569)

Discussion (1441)

Abbreviations:

4-AP, 4-aminopyridine; **AEDs**, antiepileptic drugs; ***ARA-C,*** Cytosine β-D-arabinofuranoside; ***AMPA,*** α-amino-3-hydroxy-5-methyl-4-isoxazolepropionic acid; ***AUC,*** area under curve; $[Ca^{2+}]_i$, intracellular Ca^{2+} concentration; ***CI,*** confidence intervals; ***CNQX,*** 6-cyano-7-nitroquinoxaline-2,3-dione; ***DIV,*** days in vitro; ***FLIPR,*** Fluorescent Imaging Plate Reader; ***FWHM***, full width at half maximum; ***GABA,*** γ-aminobutyric acid; ***HN***, hippocampal neurons; ***IP_3R***, inositol trisphosphate receptor; ***KAR***, kainite receptor; ***mAChRs,*** muscarinic acetylcholine receptors; ***nAChRs***, nicotinic acetylcholine receptors; ***SCOs,*** spontaneous Ca^{2+} oscillations**;** ***SKA-31***, Naphtho[1,2-*d*]thiazol-2-ylamine.

Molecular Pharmacology Fast Forward. Published on January 12, 2015 as DOI: 10.1124/mol.114.096701
This article has not been copyedited and formatted. The final version may differ from this version.

Abstract

Primary cultured hippocampal neurons (HN) form functional networks displaying synchronous Ca^{2+} oscillations (SCOs) whose patterns influence plasticity. Whether chemicals with distinct seizurogenic mechanisms differentially alter SCO patterns was investigated using mouse HN loaded with the Ca^{2+} indicator fluo-4-AM. Intracellular Ca^{2+} dynamics were recorded from 96-wells simultaneously in real-time using Fluorescent Imaging Plate Reader (FLIPR®). Although quiescent at 4 DIV, HN acquired distinctive SCO patterns as they matured to form extensive dendritic networks by 16 DIV. Challenge with kainate, a kainate receptor (KAR) agonist, 4-aminopyridine (4-AP), a K^+ channel blocker, or pilocarpine, a muscarinic acetylcholine receptor agonist caused distinct changes in SCO dynamics. Kainate at <1μM produced a rapid rise in baseline Ca^{2+} (Phase I Response) associated with high frequency and low amplitude SCOs (Phase II Response), whereas SCOs were completely repressed with ≥1μM kainate. KAR competitive antagonist CNQX (1-10μM) normalized Ca^{2+} dynamics to the pre-kainate pattern. Pilocarpine lacked Phase I activity but caused a 7-fold prolongation of Phase II SCOs without altering either their frequency or amplitude, an effect normalized by atropine (0.3-1μM). 4-AP (1-30μM) elicited a delayed Phase I response associated with persistent high frequency, low amplitude SCOs, and these disturbances were mitigated by pretreatment with the K_{Ca} activator SKA-31. Consistent with its antiepileptic and neuroprotective activities, non-selective voltage-gated Na^+ and Ca^{2+} channel blocker lamotrigine partially resolved kainate- and pilocarpine-induced Ca^{2+} dysregulation. This rapid throughput approach can discriminate among distinct seizurogenic mechanisms that alter Ca^{2+} dynamics in neuronal networks and may be useful in screening anti-epileptic drug candidates.

Molecular Pharmacology Fast Forward. Published on January 12, 2015 as DOI: 10.1124/mol.114.096701
This article has not been copyedited and formatted. The final version may differ from this version.

Introduction

Epilepsy is a complex neurological disorder which affects approximately 50 million people worldwide. It is characterized by recurrent spontaneous seizures due to neuronal hyperexcitability and hypersynchronous neuronal firing derived from various mechanisms. Seizures can cause devastating damage to the brain leading to cognitive impairment and increased risk of epilepsy (Reddy *et al.*, 2013). Despite the availability of more than 20 antiepileptic drugs (AEDs), around 30% of epilepsy patients experience refactory seizures or suffer from unacceptable drug side effects such as drowsiness, behavioral changes, memory impairment or teratogenicity (Bialer *et al.*, 2013; Bialer *et al.*, 2010; Sirven *et al.*, 2012).

Recent research in the epilepsy field is moving from a primary focus on controlling seizures to address the underlying pathophysiology. In animal models of epilepsy, patterns of dysregulated Ca^{2+} dynamics have been well established (Chen, 2012; Deshpande *et al.*, 2010; Deshpande *et al.*, 2014; McNamara *et al.*, 2006). Aberrant Ca^{2+} dynamics have been proposed to be a major if not essential contributor to seizure induction and pathophysiology (Chen, 2012; McNamara *et al.*, 2006). However, many of these studies have primarily focused on the etiological role of intracellular Ca^{2+} overload and production of reactive oxygen species (ROS) and redox-mediated damage following status epilepticus.

Primary dissociated cultures of hippocampal neurons form extensive dendritic networks with functional synapses that exhibit synchronous electrical activity that drive synchronous spontaneous Ca^{2+} oscillations (SCOs) (Bacci *et al.*, 1999; Cao *et al.*, 2012a; Dravid *et al.*, 2004b). These SCOs control the growth and functional maturation of the neural network *in vitro* by regulating Ca^{2+}-dependent pathways that influence gene transcription, metabolism

Molecular Pharmacology Fast Forward. Published on January 12, 2015 as DOI: 10.1124/mol.114.096701
This article has not been copyedited and formatted. The final version may differ from this version.

and neuronal plasticity (Lamont *et al.*, 2012; West *et al.*, 2011; Wiegert *et al.*, 2011). Recent studies have demonstrated that chemicals capable of inducing status epilepticus also alter neuronal excitability and Ca^{2+} oscillatory dynamics in hippocampal and cortical neuronal culture models (Cao *et al.*, 2014a; Cao *et al.*, 2012a; Pacico *et al.*, 2014). 4-Aminopyridine (4-AP), a nonselective K^+ channel blocker, was shown to trigger high frequency SCOs in neocortical neurons, whereas tetramethylenedisulfotetramine (TETS) or picrotoxin, inhibitors of type A γ-aminobutyric acid ($GABA_A$) receptors, both produced identical temporal changes in Ca^{2+} dynamics which included a rapid rise of baseline Ca^{2+} (termed the Phase I Response) in association with a prolonged low frequency large amplitude SCO pattern (termed the Phase II Response) in hippocampal neurons but not in neocortical neurons (Cao *et al.*, 2012a). These recent data suggest that excitotoxic chemicals that promote seizures by engaging distinct biochemical targets might be resolved by how they differentially influence neuronal Ca^{2+} dynamics and SCO. Importantly, acute alterations in SCO patterns could provide valuable leads to identify downstream signaling mechanisms that affect long-term changes in neuronal development and neuropathology (Cao *et al.*, 2014b).

In this study, we investigated whether seizurogenic chemicals with distinct primary mechanisms of excitotoxicity differentially alter Ca^{2+} dynamics and patterns of SCOs in primary hippocampal neurons (HN) that display mature neuronal network activity. The novelty to the approach was to measure changes in SCO activity before and after acute challenge of neurons loaded with Ca^{2+} indicator fluo-4-AM while continuously monitoring intracellular Ca^{2+} dynamics simultaneously from 96-wells in real-time using a Fluorescent Imaging Plate Reader (FLIPR). We report that epileptogenic compounds having known

primary excitotoxic etiologies produce distinctive alterations in Ca^{2+} dynamics, especially modified patterns of SCOs, which can be resolved using FLIPR. We further demonstrate the potential value of the rapid throughput assay in resolving and identifying anti-epileptic drug candidates.

Materials and methods

Materials

Fetal bovine serum and soybean trypsin inhibitor were obtained from Atlanta Biologicals (Norcross, GA). DNase, poly-L-lysine, cytosine arabinoside (ARA-C), Kainate, 4-aminopyridine (4-AP), 6-cyano-7-nitroquinoxaline-2,3-dione (CNQX), pilocarpine, lamotrigine, and atropine were from Sigma-Aldrich (St. Louis, MO). The anti-MAP2 antibody was from Synaptic Systems (Goettingen, Germany) and the anti-GFAP antibody was from Cell Signaling Technology (Danvers, MA, USA). The Ca^{2+} fluorescence dye Fluo-4 and Neurobasal medium were purchased from Life Technology (Grand Island, NY). SKA-31 (Naphtho[1,2-*d*]thiazol-2-ylamine) was synthesized as described previously (Sankaranarayanan *et al.*, 2009) .

Primary cultures of hippocampal neurons

Animals were treated humanely and with regard for alleviation of suffering according to protocols approved by the Institutional Animal Care and Use Committee of the University of California, Davis. Dissociated hippocampal neurons (HN) with minimal astrocyte composition were cultured as described previously (Cao *et al.*, 2012a). Briefly, neurons were dissociated from hippocampi dissected from C57BL/6J mouse pups at postnatal day 0-1 and maintained in Neurobasal complete medium [Neurobasal medium supplemented with NS21,

Molecular Pharmacology Fast Forward. Published on January 12, 2015 as DOI: 10.1124/mol.114.096701
This article has not been copyedited and formatted. The final version may differ from this version.

0.5mM L-glutamine, HEPES (Chen *et al.*, 2010)] with 5% fetal bovine serum. Dissociated hippocampal cells were plated onto poly-L-lysine (0.5mg/ml) coated clear-bottom, black wall, 96-well imaging plates (BD, Franklin Lakes, NJ, USA) at a density of $0.75x10^5$/well. After 24-48 h culture, a final concentration of 10 μM ARA-C was added to the culture medium to prevent astrocyte proliferation. The medium was changed twice a week by replacing half the volume of culture medium with serum-free Neurobasal complete medium lacking fetal bovine serum. The neurons were maintained at 37°C with 5% CO_2 and 95% humidity and measured for SCO activity at 4, 6, 9, 12, or 16 DIV.

Measurement of ynchronous Ca^{2+} oscillations (SCOs)

HN were used to investigate the basal characteristics of SCOs and how seizurogenic agents alter synchronous Ca^{2+} oscillations. This method permits simultaneous measurements of intracellular Ca^{2+} transients in intact neurons in a 96-well format as described previously (Cao *et al.*, 2012a; Cao *et al.*, 2010). Briefly, the growth medium was removed and replaced with dye loading buffer (100 μl/well) containing 4 μM Fluo-4 and 0.5% BSA in Locke's buffer consisting of (in mM) 4-(2-hydroxyethyl)-1-piperazineethanesulfonic acid (8.6), KCl (5.6), NaCl (154), glucose (5.6), $MgCl_2$ (1.0), $CaCl_2$ (2.3), and glycine (0.1), pH 7.4. After 1h incubation in dye loading buffer, the neurons were washed four times in fresh Locke's buffer (200 μl/well) and transferred to a Fluorescence Laser Plate Reader (FLIPR Tetra) (Molecular Devices, Sunnyvale, CA) incubation chamber. Baseline recording were acquired in Locke's buffer for 2-5 min followed by addition of vehicle or seizurogenic chemicals using a programmable 96-channel pipetting robotic system, and the fluorescent signals were recorded for at least an additional 30 min from a population of neurons at a central rectangle region of

Molecular Pharmacology Fast Forward. Published on January 12, 2015 as DOI: 10.1124/mol.114.096701
This article has not been copyedited and formatted. The final version may differ from this version.

each well. Although FLIPR can record the signals at a maximum speed of 8 Hz, however, at this recording speed, the fluorescence signals decrease dramatically. The duration of a typical SCO during the basal period was 10-12 s depending on the development stage of the HNs. SCO data were recorded at 1 Hz, which was sufficient to resolve these events. To measure kainate- and 4-AP-stimulated SCO properties, data acquisition was increased to 2 Hz (i.e., 0.5 s per data point), which was sufficient to resolve SCO signal whose mean duration was approximately 4 s. All pharmacological interventions were performed on mature HN cultures between 9-12 DIV by adding the inhibitors/activators 5 or 10 min before addition of the seizurogenic agent. The background fluorescence of the plate was determined from a sister well without Fluo-4 loading, and all the fluorescence signals were corrected by subtracting the plate background fluorescence. Data were presented as F/F_0. The SCO frequency and amplitude were manually counted before and after addition of the agonists/antagonists. Events having F/F_0 >0.05 units were included in the analyses of SCO frequency and amplitude.

Immunocytochemistry

HN at 6, 9 and 12 days *in vitro* (DIV) were fixed with 4% paraformaldehyde for 20 min and then permeabilized with 0.25% triton x-100 for 15 min. Following blocking with PBS with 10% BSA and 1% goat serum for 1h, cells were incubated with anti-MAP2 (1:1000) and anti-GFAP (1:500) antibodies in PBS containing 1% goat serum overnight at 4 ˚C. Cells were then incubated with Alexa Fluor 488-conjugated goat anti-guinea pig (1:500) and Alexa Fluor-568-conjugated goat anti-mouse (1:500) secondary antibodies for 1 h at room temperature. After aspiration of the secondary antibody, 0.2mg/ml Hoechst 33342 was added

Molecular Pharmacology Fast Forward. Published on January 12, 2015 as DOI: 10.1124/mol.114.096701
This article has not been copyedited and formatted. The final version may differ from this version.

to each well for 5 min to stain the nuclei. Pictures were recorded using an ImageXpress High Content Imaging System (Molecular Devices, Sunnyvale, CA) using a 10x objective with DAPI, FITC, and Texas Red filters. Nine adjacent sites (3x3), which cover ~60% of the center surface area, were imaged for each well.

Data analysis

Graphing and statistical analysis were performed using GraphPad Prism software (Version 5.0, GraphPad Software Inc., San Diego, CA). The EC_{50} and 95% confidence interval were determined by non-linear regression using GraphPad Prism software (Version 5.0, GraphPad Software Inc., San Diego, CA). Statistical significance between different groups was calculated using an ANOVA and, where appropriate, a Dunnett's multiple comparison test; *p* values below 0.05 were considered statistically significant.

Results

Developmental changes of SCOs in hippocampal neurons cultures

Hippocampal neurons (HN) were cultured in 96-well plates (initial density of 75,000 cells/well) and the neuronal maker MAP2 was used to stain and visualize cells at 6, 9, and 12 DIV. HN showed extensive dendritic networks by 6 DIV that increased in their complexity with age in culture (**Fig. 1A,** green stain). The addition of ARA-C 24-48 h post-plating limited the percentage of astrocytes in HN cultures detected with GFAP to less than 5% throughout the culture period investigated (**Fig. 1A,** red stain).

HN cultures displayed a distinctive pattern of spontaneous SCOs during the developmental window investigated (4-16 DIV). Cultures at 4 DIV displayed rare

Molecular Pharmacology Fast Forward. Published on January 12, 2015 as DOI: 10.1124/mol.114.096701
This article has not been copyedited and formatted. The final version may differ from this version.

spontaneous SCOs with very small amplitude (**Fig. 1B,** arrow). By 6 DIV, SCOs became pronounced and displayed regular periodicity and similar amplitudes across the experiment lasting at least 10 min (**Fig. 1B,** second trace and 1C). The mean duration of each SCO, calculated as full width at half maximum (FWHM, $T_{1/2}$) was significantly increased from 5 s at 4 DIV to 8.5±0.9 s at 6 DIV (mean±SD) (**Fig. 1D**). At 9 DIV average SCO amplitude continued to increase, and although their frequency only slightly increased, the temporal pattern of SCOs became more complex with increased clustering of events (**Fig 1B,** third trace). The FWHM declined to 6.4±0.7 s (**Fig. 1D**). By 12 DIV, SCO frequency continued to increase with each event having smaller but more heterogeneous amplitudes, and increased complexity in temporal patterning (**Fig. 1B,** forth trace). Thus, as the neuronal network gained morphological complexity (**Fig 1A**), SCO patterning also gained temporal complexity (**Fig. 1B&C**). The amplitude and frequency of SCOs decreased slightly by 16 DIV, although patterning remained complex (**Fig. 1B,** trace 5; **Fig. 1C**). It should be noted that although individual cultures displayed similar developmental profiles, developmental variations in SCO amplitudes and frequency were observed among the three independent cultures assessed in this study. Nevertheless, independent cultures showed consistent developmental patterns in SCO properties and served as their own baseline for comparison to subsequent pharmacological intervention.

Kainate alters Ca^{2+} dynamics and SCO patterns of HN networks

Kainate receptors (KAR) are ionotropic glutamate receptors selectively permeable to Na^+ and K^+ ions and are responsible for generating postsynaptic excitatory potentials. Although permeability to Ca^{2+} ions is usually small, it varies with subunit composition and their slow

Molecular Pharmacology Fast Forward. Published on January 12, 2015 as DOI: 10.1124/mol.114.096701
This article has not been copyedited and formatted. The final version may differ from this version.

activation and deactivation kinetics promote appreciable Ca^{2+} flux into postsynaptic neurons through NMDA receptor activation. The selective KAR agonist kainate is a naturally occurring excitatory amino acid commonly used in epilepsy research to induce seizures (Larsen *et al.*, 2011; Levesque *et al.*, 2013). After baseline recordings were completed, acute challenge of HN with a low concentration (0.1μM) of kainate produced a rapid rise in baseline cytoplasmic Ca^{2+} (termed a Phase I Response) whose magnitude was concentration-dependent and did not return to the pre-challenge baseline for the length (20 min) of the recording (**Fig. 2A**). The EC_{50} value for the kainate-induced Phase I Response was 0.38 μM (95% CI, 0.15 μM to 0.98 μM) (**Fig. 2B**). Acute challenge with low concentrations of kainate ($\leq$ 0.3 μM) also elicited a short-lived burst of high frequency SCO activity >10-fold of the initial basal activity that faded with time (termed Phase II Response) (**Fig. 2A,** traces 2&3), although kainate concentrations $\geq$ 1 μM quickly abated SCO activity altogether but induced a long-lasting global increase in intracellular Ca^{2+} (**Fig. 2A,** traces 4-6; **Fig. 2C&D**). Therefore, kainate produced a bell-shaped Phase II concentration-effect relationship on SCOs frequency. Kainate also suppressed the Phase II Response (SCOs amplitude) in a concentration-dependent manner with a half maximal inhibition constant of 0.11 μM (0.08-0.14 μM, 95%CI, **Fig. 2D**).

To examine whether part or all of the Phase I and II Responses observed with kainate are mediated by KAR, the cells were pretreated for 5 min with CNQX, a selective α-amino-3-hydroxy-5-methyl-4-isoxazolepropionic acid (AMPA) receptor / KAR antagonist, prior to challenge with kainate (0.3 μM) as described above. CNQX prevented the kainate-triggered Phase I Response (at 10 μM) (**Fig. 3A&B**), and at a concentration of 3 μM,

Molecular Pharmacology Fast Forward. Published on January 12, 2015 as DOI: 10.1124/mol.114.096701
This article has not been copyedited and formatted. The final version may differ from this version.

abated the Phase II Response (kainate-induced reduction in SCO frequency) (**Fig. 3A&C**). CNQX pretreatment also greatly ameliorated the Phase II decrease in SCO amplitude produced by kainate (from 77% to 6.7% reduction in the original baseline amplitude) (**Fig. 3D**). CNQX at concentrations > 1 μM also eliminated basal SCOs activity (Fig 3A, traces 3-5, time scale 300-600 s).

Pilocarpine alters SCO patterns in a manner distinct from kainate

Pilocarpine, a non-selective muscarinic acetylcholine receptor (mAChR) agonist, has been used to develop animal seizure models in rodents in order to study human epilepsy (Curia *et al.*, 2008; de Araujo Furtado *et al.*, 2012). Pilocarpine was chosen to investigate whether excitatory agonists that differ in their underlying mechanisms (activation of KAR *vs*. mAChR) induce distinct SCOs responses in HN cultures. In contrast to kainate, pilocarpine (10-100 μM) produced a concentration- and time-dependent prolongation of SCOs (calculated as FWHM; $T_{1/2}$) with an EC_{50} of 14.2 μM (8.8-22.7 μM, 95%CI) (**Fig. 4A-C**), without affecting SCO frequencies and amplitudes (**Fig. 4D**). The potency is similar to pilocarpine action on the inhibition of [^{3}H](R)-QNB binding to muscarinic receptor in rat brain membranes (IC_{50}=7.6 μM) (Messer *et al.*, 1992).

To further investigate whether HN responses to pilocarpine are primarily mediated by mAChR over-activation, the cells were pretreated with atropine, a competitive mAChR antagonist, for 10 min before challenge with 10 μM pilocarpine. Atropine completely prevented pilocarpine-induced prolongation of the SCO transients (**Fig. 5**). Atropine itself had no significant effect on the basal SCO patterns.

Molecular Pharmacology Fast Forward. Published on January 12, 2015 as DOI: 10.1124/mol.114.096701
This article has not been copyedited and formatted. The final version may differ from this version.

Block of potassium channels with 4-AP uniquely alters Ca^{2+} dynamics in HN cultures

We next investigated the influence of a universal voltage-dependent potassium (Kv) channel blocker 4-aminopyridine (4-AP), which has been widely used as an *in vivo* and *in vitro* model of epilepsy (Avoli *et al.*, 2002; Kobayashi *et al.*, 2008). Our goal was to determine if yet another mode of action leading to excitation (inhibition of K_V currents) produced SCO patterns different from those observed in cultured HN treated with kainate or pilocarpine.

Interestingly, 4-AP (> 1μM) produced a Phase I rise in baseline Ca^{2+} whose overshoot was significantly delayed compared to that produced by kainate (**Fig. 6A, traces 3-6**) with an EC_{50} of 1.76 μM (1.21 to 2.54 μM; 95% CI). Unlike either kainate or pilocarpine, 4-AP produced a long-lasting high-frequency Phase II response with persistent high frequency (>10-fold baseline) and 3-fold lower amplitude of SCOs (**Fig. 6C&D**). The EC_{50} for increased SCOs frequency was 2.33 μM (1.30-4.18 μM, 95%CI), and the IC_{50} value for 4-AP attenuation of SCOs amplitude was 1.33 μM (1.05-1.74 μM, 95%CI) (**Fig. 6C&D**).

SKA-31 is an activator of Ca^{2+}-activated intermediate-conductance KCa3.1 and small conductance KCa2 channels, which has been shown to suppress electroshock-induced seizures and improve motor deficits in a model of ataxia (Sankaranarayanan *et al.*, 2009; Shakkottai *et al.*, 2011). Pretreatment of HN cultures with SKA-31 (10 μM) for 5 min normalized the Phase I Response to 4-AP (3 μM) and partially attenuated the high frequency response and decline in amplitude in Phase II by approximately 50% each (**Fig. 7C&D**). To achieve such efficacy, SKA-31 (10 μM) also suppressed basal SCO activity (**Fig. 7A, fifth trace**).

Molecular Pharmacology Fast Forward. Published on January 12, 2015 as DOI: 10.1124/mol.114.096701
This article has not been copyedited and formatted. The final version may differ from this version.

Pharmacological antagonism with lamotrigine prevents pilocarpine- and kainate-triggered Ca^{2+} dysregulation

Next we tested whether altered Ca^{2+} dynamics elicited by pilocarpine agonism of mAChRs in the HN culture model could be prevented by a pharmacological action not mediated by direct receptor-site competition. The anti-epileptic drug lamotrigine (LTG), a low affinity Na^{+} channel blocker preferentially binds to the inactive state of the sodium channels with K_d values of ~10μ M (200 times less potent than block of resting channels) (Kuo *et al.*, 1997). LTG (3-10 μM) prevented the prolonged SCO duration elicited by pilocarpine (10 μM) in HN cultures (**Fig. 8A-C**).

LTG was also effective at suppressing Phase I and Phase II responses triggered by kainate (0.3 μM); however, much higher LTG concentrations were needed (30-100 μM), levels that also completely blocked baseline SCO activity **(Fig. 9A-D)**.

Discussion

Real-time multicellular imaging of Ca^{2+} dynamics in neuronal cultures that have established a high degree of synaptic connectivity provides a medium to high throughput *in vitro* approach for understanding how excitotoxicants of known mechanisms influence network connectivity at the level of local circuits. The major finding here is that distinct seizurogenic mechanisms differentially alter patterns of SCO activity measured in primary hippocampal neuronal circuits. As HN developed more complex morphology *in vitro,* the temporal pattern and amplitude of SCOs also became more complex. SCOs in cultured neuronal networks are dependent on action potentials and the release of synaptic

Molecular Pharmacology Fast Forward. Published on January 12, 2015 as DOI: 10.1124/mol.114.096701
This article has not been copyedited and formatted. The final version may differ from this version.

neurotransmitter vesicles (Dravid *et al.*, 2004b). A number of studies have suggested that SCO activity is highly dependent on the balance of ongoing excitatory ionotropic glutamatergic and inhibitory GABAergic neurotransmission within the neuronal network (George *et al.*, 2009, Dravid *et al.*, 2004b; Koga *et al.*, 2010; Pacico *et al.*, 2014). In addition to ionotropic Glu receptors, both type I and type II metabotropic Glu receptors (mGluRs) also modulate SCO patterns (Dravid *et al.*, 2004b; Koga *et al.*, 2010). For example, positive allosteric modulators of $GABA_A$ receptors ($GABA_AR$), such as diazepam or allopregnanolone, decreased SCO amplitude and frequency, and acted synergistically (Cao *et al.*, 2012a). In contrast, suppression of $GABA_A$ receptor function with picrotoxin (PTX), bicuculline, or tetramethylenedisulfotetramine (TETS) evoked characteristic Phase I (rapid elevation of cytosolic Ca^{2+} level) and Phase II Responses (decreased SCO frequency and increased SCO amplitude) (Cao *et al.*, 2012a). Importantly, despite the distinct molecular mechanisms by which these three chemicals interfere with $GABA_AR$ neurotransmission, they modify SCO patterns in an indistinguishable manner that differs from the excitotoxicants tested here (KA, 4-AP, pilocarpine) that target distinct receptor classes.

Although KA produced a prominent Phase I response at the lowest concentration tested (0.1μM), it was associated with high-frequency bursts of SCO having reduced amplitudes that eventually failed. In marked contrast to TETS, higher concentrations of KA expedited SCO failure while maintaining chronically elevated cytoplasmic Ca^{2+}. The different patterns of Ca^{2+} dysregulation seen with KA undoubtedly stem from the enhanced Ca^{2+} entry mediated by prolonged activation of ionotropic GluR signaling compared to the indirect influence of impaired inhibitory inputs on Glu neurotransmission mediated by TETS (Cao *et*

Molecular Pharmacology Fast Forward. Published on January 12, 2015 as DOI: 10.1124/mol.114.096701
This article has not been copyedited and formatted. The final version may differ from this version.

al., 2012a). The observation that CNQX ameliorates KA-induced Ca^{2+} dysregulation supports our interpretation. The SCOs in primary cultured neurons are dependent on Ca^{2+} release from intracellular Ca^{2+} stores. Thapsigargin, which depletes Ca^{2+} stores, suppresses SCOs in primary cultured neurons and inhibition of 1,4,5-inositol trisphosphate receptors completely abrogated Ca^{2+} oscillations (Dravid *et al.*, 2004b). KA produced a persistent Ca^{2+} rise that stems from both Ca^{2+} entry and Ca^{2+} release from intracellular Ca^{2+} stores, and likely to rapidly deplete the latter (Kocsis *et al.*, 1993; Lee *et al.*, 2000). The loss of dynamic regulation between Ca^{2+} entry and Ca^{2+} stores could explain the rapid loss of SCOs in HN exposed to KA.

It further follows that non-selective K^+ channel negative modifiers, including 4-AP, should enhance neuronal excitability and alter Ca^{2+} dynamics in concert (Cao *et al.*, 2014a; Pacico *et al.*, 2014). The present results also reveal that in contrast to both KA and TETS (Cao *et al.*, 2012a), inhibition of K^+ channels produces a delayed Phase I response that is associated with very high-frequency SCOs that persist for more than 20 minutes. SKA-31, a selective activator of KCa2 and KCa3.1 channels (Sankaranarayanan *et al.*, 2009) afforded protection to 4-AP induced Ca^{2+} dysregulation. Small- and intermediate-conductance Ca^{2+}-activated K^+ channels regulate membrane potential and modulate Ca^{2+}-signaling cascades. For example KCa2 channels underlie the apamin-sensitive medium afterhyperpolarization currents and thereby regulate neuronal firing frequency and neurotransmitter release (Stocker, 2004; Wulff *et al.*, 2007). Thus, in contrast to ligand-gated receptor mechanisms mediated by $GABA_AR$ block or KAR activation described above, 4-AP excites both excitatory and inhibitory pathways in the networks that leads to increased firing

Molecular Pharmacology Fast Forward. Published on January 12, 2015 as DOI: 10.1124/mol.114.096701
This article has not been copyedited and formatted. The final version may differ from this version.

frequency of action potentials across the entire network that could explain the persistent high frequency SCO activity seen in HN cultures. We recently demonstrated that SKA-19, a dual function $Na_v1.2$ inhibitor and KCa2 activator, normalizes 4-AP Ca^{2+} responses and protected against seizures in the various rodent models of epilepsy (Coleman *et al.*, 2014).

In the CA3 region of adult rat hippocampal slices, pilocarpine induced both theta rhythm and synchronous ictal discharges (Hadar *et al.*, 2002). Although the basal SCO activity produced by HN cultures used in our studies failed to respond to challenge with atropine, exogenous addition of ACh modulated SCO behavior in a complex manner and was mediated by muscarinic receptor (mAChR) activation (data not shown). It is therefore not unexpected that the mAChR agonist pilocarpine modulated SCO activity in a unique manner that could be completely normalized by pretreatment with atropine. Collectively these data further support the interpretation that basal SCO activity is mediated by excitatory Glu neurotransmission, but can be modulated by mAChR activation. Pilocarpine could mediate significant prolongation of SCO events by activating excitatory Gαq signaling (mediated by subtype 1, 3 and 5 mAChRs), activating inhibitory Gαi signaling (mediated by type 2 and 4 mAChRs), or a balance of both ACh pathways (Brown, 2010; Lucas-Meunier *et al.*, 2003). Since pilocarpine does not discriminate among mAChR subtypes further studies are needed to resolve which pathway predominates in prolonging SCOs.

Collectively these data show that modification of Ca^{2+} dynamics and SCO patterns depends on the principal receptor-mediated mechanisms targeted by seizurogenic excitotoxicants, and each pattern of excitotoxic response can be ameliorated by pretreatment of the HN cultures with an agent that specifically antagonizes the excitotoxicant at their

Molecular Pharmacology Fast Forward. Published on January 12, 2015 as DOI: 10.1124/mol.114.096701
This article has not been copyedited and formatted. The final version may differ from this version.

respective receptor target. Furthermore, we also demonstrate that the clinically used anticonvulsant lamotrigine antagonizes both kainate- and pilocarpine-induced Ca^{2+} responses at therapeutic concentrations. This is consistent with previous studies demonstrating that the low affinity Na^{+} channel antagonist CBZ antagonized pilocarpine-induced status epilepticus (Morrisett *et al.*, 1987) and neuronal cell death (Cunha *et al.*, 2009). Both CBZ and LTG also suppress KA-triggered status epilepticus (Czuczwar *et al.*, 1982; Wang *et al.*, 2000) and neuronal cell death (Das *et al.*, 2010; Halbsgut *et al.*, 2013; Park *et al.*, 2013).

It is tempting to suggest that differential patterns in Ca^{2+} dynamics and SCO patterns elicited by $GABA_AR$ blockers, K^{+} channel blockers, ionotropic GluR or mAChR agonists could influence patterns of seizure onset and progression, and/or the extent of post-seizure neuropathology. For example, TETS and PTX alter Ca^{2+} dynamics and SCO patterns indistinguishably (Cao *et al.*, 2012). In mice, intraperitoneal injections of TETS or PTX cause similar sequences of immobility, myoclonic body jerks, clonic seizures of the forelimbs and/or hindlimbs, tonic seizures (falling on the side followed by forelimb tonic contraction and hindlimb tonic extension, and eventually death (Zolkowska *et al.*, 2012). Systematic TETS exposures that are not fatal produce transient gliosis (2-3 days post-exposure) in both the hippocampus and cortex without evidence of cellular injury and neurodegeneration (Vito *et al.*, 2014; Zolkowska *et al.*, 2012). In contrast, administration of KA to rats induces a distinct progression of symptoms including staring episodes, head bobbing, numerous wet dog shakes, and isolated limbic motor seizures that increase in frequency, eventually leading to status epilepticus (Scerrati *et al.*, 1986), which resemble the clinic features of human temporal lobe epilepsy (Ben-Ari, 1985). *In vivo* exposures to KA are known to rapidly induce

Molecular Pharmacology Fast Forward. Published on January 12, 2015 as DOI: 10.1124/mol.114.096701
This article has not been copyedited and formatted. The final version may differ from this version.

neurodegeneration that is both persistent and progressive (Bhowmik *et al.*, 2014; Pritt *et al.*, 2014; Reddy *et al.*, 2013). The pilocarpine seizure model displays distinct seizure behavior compared to TETS/PTX or KA. Systemic administration of pilocarpine progresses from staring spells, limbic gustatory automatisms, and motor limbic seizures that progressively developed into limbic SE that last for several hours. Pilocarpine-induced SE causes massive neuronal damage when examined at 24 to 72 h (Turski *et al.*, 1986; Turski *et al.*, 1984). In the pilocarpine epileptic animal model, pre-treatment with atropine has been shown to normalize pilocarpine-induced temporal lobe epilepsy as well as neuronal death (Curia *et al.*, 2008; Jope *et al.*, 1986; Morrisett *et al.*, 1987).

In summary, we have shown the developmental progression of SCO patterns in dissociated HN cultures can be measured with sufficient temporal resolution using 96-well parallel processing on the FLIPR platform. Our approach permits detailed analysis of how HN networks respond to acute exposure to excitotoxicants by measuring their basal cytoplasmic Ca^{2+} concentrations (i.e., Ca^{2+} dynamics) as well as SCO patterns in real-time. We discovered that seizurogenic chemicals that engage distinct receptor targets produce distinct changes in Ca^{2+} dynamics and SCO patterns and, therefore, may serve as valuable rapid screening tool for identifying and classifying excitotoxicity of potential seizurogenic agents. Importantly, this approach is capable of high throughput discovery of anticonvulsants. The method also lends itself for studies of developmental neurotoxicants (Cao *et al.*, 2014b) and those that promote neurodegeneration.

Molecular Pharmacology Fast Forward. Published on January 12, 2015 as DOI: 10.1124/mol.114.096701
This article has not been copyedited and formatted. The final version may differ from this version.

Author contributions:

Participated in research design: Cao, Z., Wulff, H and Pessah, I.N.

Conducted experiments: Cao, Z., Cui, Y. and Hulsizer, S.

Contributed new reagents or analytic tools: Wulff, H.

Performed data analysis: Cao. Z., Zou, X, and Cui, Y.

Wrote or contributed to the writing of the manuscript: Cao, Z., Lein, P.J., Wulff, H., and Pessah, I.N.

References

Avoli M, D'Antuono M, Louvel J, Kohling R, Biagini G, Pumain R, *et al.* (2002). Network and pharmacological mechanisms leading to epileptiform synchronization in the limbic system in vitro. *Prog Neurobiol* 68(3): 167-207.

Bacci A, Verderio C, Pravettoni E, Matteoli M (1999). Synaptic and intrinsic mechanisms shape synchronous oscillations in hippocampal neurons in culture. *Eur J Neurosci* 11(2): 389-397.

Ben-Ari Y (1985). Limbic seizure and brain damage produced by kainic acid: mechanisms and relevance to human temporal lobe epilepsy. *Neuroscience* 14(2): 375-403.

Bhowmik M, Saini N, Vohora D (2014). Histamine H3 receptor antagonism by ABT-239 attenuates kainic acid induced excitotoxicity in mice. *Brain Res* 1581: 129-140.

Bialer M, Johannessen SI, Levy RH, Perucca E, Tomson T, White HS (2013). Progress report on new antiepileptic drugs: a summary of the Eleventh Eilat Conference (EILAT XI). *Epilepsy Res* 103(1): 2-30.

Bialer M, White HS (2010). Key factors in the discovery and development of new antiepileptic drugs. *Nat Rev Drug Discov* 9(1): 68-82.

Brown DA (2010). Muscarinic acetylcholine receptors (mAChRs) in the nervous system: some functions and mechanisms. *J Mol Neurosci* 41(3): 340-346.

Cao Z, Cui Y, Busse E, Mehrotra S, Rainier JD, Murray TF (2014a). Gambierol inhibition of voltage-gated potassium channels augments spontaneous Ca^{2+} oscillations in cerebrocortical neurons. *J Pharmacol Exp Ther* 350(3): 615-623.

Cao Z, Cui Y, Nguyen HM, Jenkins DP, Wulff H, Pessah, IN (2014b). Nanomolar bifenthrin alters synchronous Ca^{2+} oscillations and cortical neuron development independent of sodium channel activity. *Molec Pharmacol* 85: 630-639.

Cao Z, Hammock BD, McCoy M, Rogawski MA, Lein PJ, Pessah IN (2012a). Tetramethylenedisulfotetramine alters Ca^{2+} dynamics in cultured hippocampal neurons: mitigation by NMDA receptor blockade and GABA(A) receptor-positive modulation. *Toxicol Sci* 130(2): 362-372.

Cao Z, LePage KT, Frederick MO, Nicolaou KC, Murray TF (2010). Involvement of caspase activation in azaspiracid-induced neurotoxicity in neocortical neurons. *Toxicol Sci* 114(2): 323-334.

Cao Z, Shafer TJ, Murray TF (2011). Mechanisms of pyrethroid insecticide-induced stimulation of calcium influx in neocortical neurons. *J Pharmacol Exp Ther* 336(1): 197-205.

Chen Y (2012). Organophosphate-induced brain damage: mechanisms, neuropsychiatric and

neurological consequences, and potential therapeutic strategies. *Neurotoxicology* 33(3): 391-400.

Chen Y, Tassone F, Berman RF, Hagerman PJ, Hagerman RJ, Willemsen R, *et al.* (2010). Murine hippocampal neurons expressing Fmr1 gene premutations show early developmental deficits and late degeneration. *Hum Mol Genet* 19(1): 196-208.

Coleman N, Nguyen HM, Cao Z, Brown BM, Jenkins DP, Zolkowska D, *et al.* (2014). The Riluzole Derivative 2-Amino-6-trifluoromethylthio-benzothiazole (SKA-19), a Mixed K2 Activator and Na Blocker, is a Potent Novel Anticonvulsant. *Neurotherapeutics*.

Cunha AO, Mortari MR, Liberato JL, dos Santos WF (2009). Neuroprotective effects of diazepam, carbamazepine, phenytoin and ketamine after pilocarpine-induced status epilepticus. *Basic Clin Pharmacol Toxicol* 104(6): 470-477.

Curia G, Longo D, Biagini G, Jones RS, Avoli M (2008). The pilocarpine model of temporal lobe epilepsy. *J Neurosci Methods* 172(2): 143-157.

Czuczwar SJ, Turski L, Kleinrok Z (1982). Anticonvulsant action of phenobarbital, diazepam, carbamazepine, and diphenylhydantoin in the electroshock test in mice after lesion of hippocampal pyramidal cells with intracerebroventricular kainic acid. *Epilepsia* 23(4): 377-382.

Das A, McDowell M, O'Dell CM, Busch ME, Smith JA, Ray SK, *et al.* (2010). Post-treatment with voltage-gated Na(+) channel blocker attenuates kainic acid-induced apoptosis in rat primary hippocampal neurons. *Neurochem Res* 35(12): 2175-2183.

de Araujo Furtado M, Rossetti F, Chanda S, Yourick D (2012). Exposure to nerve agents: from status epilepticus to neuroinflammation, brain damage, neurogenesis and epilepsy. *Neurotoxicology* 33(6): 1476-1490.

Deshpande LS, Carter DS, Blair RE, DeLorenzo RJ (2010). Development of a prolonged calcium plateau in hippocampal neurons in rats surviving status epilepticus induced by the organophosphate diisopropylfluorophosphate. *Toxicol Sci* 116(2): 623-631.

Deshpande LS, Carter DS, Phillips KF, Blair RE, DeLorenzo RJ (2014). Development of status epilepticus, sustained calcium elevations and neuronal injury in a rat survival model of lethal paraoxon intoxication. *Neurotoxicology* 44C: 17-26.

Dravid SM, Baden DG, Murray TF (2004a). Brevetoxin activation of voltage-gated sodium channels regulates Ca dynamics and ERK1/2 phosphorylation in murine neocortical neurons. *J Neurochem* 89(3): 739-749.

Dravid SM, Murray TF (2004b). Spontaneous synchronized calcium oscillations in neocortical neurons in the presence of physiological [Mg(2+)]: involvement of AMPA/kainate and metabotropic glutamate receptors. *Brain Res* 1006(1): 8-17.

Frega M, Pasquale V, Tedesco M, Marcoli M, Contestabile A, Nanni M, *et al.* (2012). Cortical cultures coupled to micro-electrode arrays: a novel approach to perform in vitro excitotoxicity testing. *Neurotoxicol Teratol* 34(1): 116-127.

George J, Dravid SM, Prakash A, Xie J, Peterson J, Jabba SV, *et al.* (2009). Sodium channel activation augments NMDA receptor function and promotes neurite outgrowth in immature cerebrocortical neurons. *J Neurosci* 29(10): 3288-3301.

Hadar EJ, Yang Y, Sayin U, Rutecki PA (2002). Suppression of pilocarpine-induced ictal oscillations in the hippocampal slice. *Epilepsy Res* 49(1): 61-71.

Halbsgut LR, Fahim E, Kapoor K, Hong H, Friedman LK (2013). Certain secondary antiepileptic drugs can rescue hippocampal injury following a critical growth period despite poor anticonvulsant activity and cognitive deficits. *Epilepsy Behav* 29(3): 466-477.

Jope RS, Morrisett RA, Snead OC (1986). Characterization of lithium potentiation of pilocarpine-induced status epilepticus in rats. *Exp Neurol* 91(3): 471-480.

Kobayashi K, Nishizawa Y, Sawada K, Ogura H, Miyabe M (2008). K(+)-channel openers suppress epileptiform activities induced by 4-aminopyridine in cultured rat hippocampal neurons. *J Pharmacol Sci* 108(4): 517-528.

Kocsis JD, Rand MN, Chen B, Waxman SG, Pourcho R (1993). Kainate elicits elevated nuclear calcium signals in retinal neurons via calcium-induced calcium release. *Brain Res* 616(1-2): 273-282.

Koga K, Iwahori Y, Ozaki S, Ohta H (2010). Regulation of spontaneous Ca(2+) spikes by metabotropic glutamate receptors in primary cultures of rat cortical neurons. *J Neurosci Res* 88(10): 2252-2262.

Kuo CC, Lu L (1997). Characterization of lamotrigine inhibition of Na+ channels in rat hippocampal neurones. *Br J Pharmacol* 121(6): 1231-1238.

Lamont MG, Weber JT (2012). The role of calcium in synaptic plasticity and motor learning in the cerebellar cortex. *Neurosci Biobehav Rev* 36(4): 1153-1162.

Larsen AM, Bunch L (2011). Medicinal chemistry of competitive kainate receptor antagonists. *ACS Chem Neurosci* 2(2): 60-74.

Lee YH, Fang KM, Yang CM, Hwang HM, Chiu CT, Tsai W (2000). Kainic acid-induced neurotrophic activities in developing cortical neurons. *J Neurochem* 74(6): 2401-2411.

Levesque M, Avoli M (2013). The kainic acid model of temporal lobe epilepsy. *Neurosci Biobehav Rev* 37(10 Pt 2): 2887-2899.

Lucas-Meunier E, Fossier P, Baux G, Amar M (2003). Cholinergic modulation of the cortical neuronal network. *Pflugers Arch* 446(1): 17-29.

McNamara JO, Huang YZ, Leonard AS (2006). Molecular signaling mechanisms underlying epileptogenesis. *Sci STKE* 2006(356): re12.

Messer WS, Jr., Ngur DO, Abuh YF, Dokas LA, Ting SM, Hacksell U, *et al.* (1992). Stereoselective binding and activity of oxotremorine analogs at muscarinic receptors in rat brain. *Chirality* 4(8): 463-468.

Morrisett RA, Jope RS, Snead OC, 3rd (1987). Effects of drugs on the initiation and maintenance of status epilepticus induced by administration of pilocarpine to lithium-pretreated rats. *Exp Neurol* 97(1): 193-200.

Pacico N, Mingorance-Le Meur A (2014). New in vitro phenotypic assay for epilepsy: fluorescent measurement of synchronized neuronal calcium oscillations. *PLoS One* 9(1): e84755.

Park HJ, Kim SK, Chung JH, Kim JW (2013). Protective effect of carbamazepine on kainic acid-induced neuronal cell death through activation of signal transducer and activator of transcription-3. *J Mol Neurosci* 49(1): 172-181.

Pritt ML, Hall DG, Jordan WH, Ballard DW, Wang KK, Muller UR, *et al.* (2014). Initial Biological Qualification of SBDP-145 as a Biomarker of Compound-Induced Neurodegeneration in the Rat. *Toxicol Sci* 141(2): 398-408.

Reddy DS, Kuruba R (2013). Experimental models of status epilepticus and neuronal injury for evaluation of therapeutic interventions. *Int J Mol Sci* 14(9): 18284-18318.

Sankaranarayanan A, Raman G, Busch C, Schultz T, Zimin PI, Hoyer J, *et al.* (2009). Naphtho[1,2-d]thiazol-2-ylamine (SKA-31), a new activator of KCa2 and KCa3.1 potassium channels, potentiates the endothelium-derived hyperpolarizing factor response and lowers blood pressure. *Mol Pharmacol* 75(2): 281-295.

Scerrati M, Onofrj M, Pacifici L, Pola P, Ramacci MT, Rossi GF (1986). Electrocerebral and behavioural analysis of systemic kainic acid-induced epilepsy in the rat. *Drugs Exp Clin Res* 12(8): 671-680.

Shakkottai VG, do Carmo Costa M, Dell'Orco JM, Sankaranarayanan A, Wulff H, Paulson HL (2011). Early changes in cerebellar physiology accompany motor dysfunction in the polyglutamine disease spinocerebellar ataxia type 3. *J Neurosci* 31(36): 13002-13014.

Sirven JI, Noe K, Hoerth M, Drazkowski J (2012). Antiepileptic drugs 2012: recent advances and trends. *Mayo Clin Proc* 87(9): 879-889.

Stocker M (2004). Ca(2+)-activated K+ channels: molecular determinants and function of the SK family. *Nat Rev Neurosci* 5(10): 758-770.

Tanaka T, Saito H, Matsuki N (1996). Intracellular calcium oscillation in cultured rat hippocampal neurons: a model for glutamatergic neurotransmission. *Jpn J Pharmacol* 70(1): 89-93.

Turski L, Cavalheiro EA, Sieklucka-Dziuba M, Ikonomidou-Turski C, Czuczwar SJ, Turski WA (1986). Seizures produced by pilocarpine: neuropathological sequelae and activity of glutamate decarboxylase in the rat forebrain. *Brain Res* 398(1): 37-48.

Turski WA, Cavalheiro EA, Bortolotto ZA, Mello LM, Schwarz M, Turski L (1984). Seizures produced by pilocarpine in mice: a behavioral, electroencephalographic and morphological analysis. *Brain Res* 321(2): 237-253.

Vito ST, Banks CN, Iceoglu B, Bruun DA, Zolkowska D, McCoy MR, *et al.* (2014). Post-exposure administration of diazepam combined with soluble epoxide hydrolase inhibition stops seizures and modulates neuroinflammation in a murine model of acute TETS intoxication. . *Toxicol Appl Pharmacol* In Press.

Wang L, Zuo CH, Zhao DY, Wu XR (2000). Brain distribution and efficacy of carbamazepine in kainic acid induced seizure in rats. *Brain Dev* 22(3): 154-157.

West AE, Greenberg ME (2011). Neuronal activity-regulated gene transcription in synapse development and cognitive function. *Cold Spring Harb Perspect Biol* 3(6).

Wiegert JS, Bading H (2011). Activity-dependent calcium signaling and ERK-MAP kinases in neurons: a link to structural plasticity of the nucleus and gene transcription regulation. *Cell Calcium* 49(5): 296-305.

Wulff H, Kolski-Andreaco A, Sankaranarayanan A, Sabatier JM, Shakkottai V (2007). Modulators of small- and intermediate-conductance calcium-activated potassium channels and their therapeutic indications. *Curr Med Chem* 14(13): 1437-1457.

Zolkowska D, Banks CN, Dhir A, Inceoglu B, Sanborn JR, McCoy MR, *et al.* (2012). Characterization of seizures induced by acute and repeated exposure to tetramethylenedisulfotetramine. *J Pharmacol Exp Ther* 341(2): 435-446.

Footnotes

This research was supported by the CounterACT Program, National Institutes of Health Office of the Director, and the National Institute of Neurological Disorders and Stroke [Grant NS079202]; the National Institute of Environmental Health Sciences [Grant 1R01 ES020392]; the Natural Science Foundation of China [Grant 81473539], the Jiangsu Provincial Natural Science Foundation [Grant BK20141357] and the Project Program of State Key Laboratory of Natural Medicines, China Pharmaceutical University [Grant SKLNMZZJQ201402].

Molecular Pharmacology Fast Forward. Published on January 12, 2015 as DOI: 10.1124/mol.114.096701
This article has not been copyedited and formatted. The final version may differ from this version.

Legends for figures

Figure 1|Patterns of spontaneous synchronous calcium oscillations (SCOs) at defined developmental stages of primary cultured hippocampal neurons (HN) in culture. A, Representative micrographs showing immunofluorescence staining of MAP2 and GFAP in HN cultures at 6, 9, 12 DIV. B, Representative traces of the SCOs in HN cultures at specified DIV. C, Quantification of the SCOs frequency and amplitude in HN cultured at specified DIV. D, Quantification of full width at half maximum (FWHM) of SCOs generated by HN cultures at specified DIV. Each data point represents mean±SD from at least 5 wells and the experiments were repeated three times.

Figure 2 |Kainate (KA) challenge rapidly alters Ca^{2+} dynamics in 11 DIV HN cultures. A, Representative traces of KA-induced alterations in Ca^{2+} dynamics 11 DIV HN. KA produced an immediate intracellular Ca^{2+} rise (Phase I) and a subsequent high frequency, low amplitude pattern of SCOs (Phase II). The integrated Ca^{2+} phase I response (AUC) was calculated from the initial 5 min after addition of KA to the culture medium. The phase II response was calculated from a period 10-15 min after addition of KA to the culture medium. B, KA-triggered Phase I Ca^{2+} response was concentration dependent with an EC_{50} value of 0.38μM (0.15-0.8μM, 95%CI). C, KA induced a biphasic response on the SCOs frequency. D, KA caused a concentration dependent decrease on the mean amplitude of the SCOs with an IC_{50} value of 0.11μM (0.077-0.14μM, 95%CI). Each data point represents at least four replicates and the experiments were repeated in two independent cultures with similar results.

Figure 3 |CNQX normalized KA-induced Ca^{2+} response in 9 DIV HN cultures. A, Representative traces for CNQX action on KA-induced Ca^{2+} responses. B, CNQX

ameliorated KA-induced acute Phase I Ca^{2+} responses in a concentration-dependent manner. C, CNQX suppressed KA-induced Phase II responses by increasing the frequency of Ca^{2+} oscillations. D, CNQX also reversed KA-induced decreases in the amplitude of Ca^{2+} oscillations. Each data point represents at least four replicates and the experiments were repeated twice in independent cultures with similar results. (**, $p<0.01$, KA vs Veh; ##, $p<0.01$, CNQX+KA vs KA)

Figure 4 |Pilocarpine elicited unique modification of SCO properties in 9 DIV HN cultures. A, Representative traces of pilocarpine-induced Ca^{2+} responses as a function of time in 9 DIV HN cultures. Although pilocarpine did not elicit a Phase I response, it significantly prolonged SCO full width at half maximum (FWHM) in cultured HN. B, Expanded traces representative of pilocarpine-induced Phase II Ca^{2+} responses. C, Concentration-response relationship for pilocarpine-induced prolongation of SOCs (calculated from FWHM of the SCOs). D, Pilocarpine had no effect on the SCOs frequency and amplitude. Each data point represents at least four replicates and the experiments were repeated in three independent cultures with similar results.

Figure 5 |Atropine normalized pilocarpine (10μM)-induced Ca^{2+} response in 9 DIV HN cultures. A, Representative traces showing atropine's action on pilocarpine-induced Ca^{2+} responses. B, Expanded representative traces showing atropine's action on pilocarpine-induced Ca^{2+} responses. C, Atropine reversed pilocarpine-induced prolongation of SCO lifetime. Each data point represents at least three replicates and the experiments were repeated twice in independent cultures with similar results. (**, $p<0.01$, pilocarpine vs Veh; ##, $p<0.01$, pilocarpine+atropine vs pilocarpine)

Molecular Pharmacology Fast Forward. Published on January 12, 2015 as DOI: 10.1124/mol.114.096701
This article has not been copyedited and formatted. The final version may differ from this version.

Figure 6 |4-AP alters Ca^{2+} dynamics and SCO in 10 DIV HN cultures. A, Representative traces of 4-AP-triggered Ca^{2+} responses in HN cultures at 10 DIV. 4-AP produced an immediate intracellular Ca^{2+} rise (Phase I) and concomitant high frequent SCO patterns of low amplitude (Phase II). The integrated Ca^{2+} signals (Phase I responses, AUC) were calculated from the initial 5 min after addition of 4-AP. The Phase II responses were calculated from the 5 min period between 10 and 15 min after addition of 4-AP. B, 4-AP caused an acute concentration-dependent rise in cytoplasmic Ca^{2+} with an EC_{50} value of 1.76μM (1.21-4.54μM, 95%CI). C, 4-AP increased SCO frequency with an EC_{50} value of 2.33μM (1.30-4.18μM, 95%CI). D, 4-AP elicited a concentration-dependent decrease in mean SCO amplitude with an IC_{50} value of 1.33μM (1.05-1.74μM, 95%CI). Each data point represents at least four replicates and the experiments were repeated in two independent cultures with similar results.

Figure 7 |SKA-31 normalized 4-AP (3μM) triggered dysregulation of Ca^{2+} dynamics in HN cultures at 9 DIV. A, Representative traces showing how SKA-31 influenced 4-AP-triggered Ca^{2+} dynamics. B, SKA-31 attenuated 4-AP-induced acute rise in cytoplasmic Ca^{2+}. C, SKA-31 attenuated 4-AP-triggered increases in SCO frequency. D, SKA-31 attenuated 4-AP-induced decreases in SCO amplitude. Each data point represents at least three replicates and the experiments were repeated twice in independent cultures with similar results. (**, $p<0.01$, 4-AP vs Veh; $^{\#\#}$, $p<0.01$, SKA 31+4-AP vs 4-AP)

Figure 8 |Lamotrigine normalized KA (0.3μM)-induced Ca^{2+} responses in 9 DIV HN cultures. A, Representative traces showing how lamotrigine (LTG) influences KA-induced Ca^{2+} responses. B, LTG ameliorated KA-induced acute rise in cytoplasmic Ca^{2+} in a

concentration-dependent manner. C, LTG suppressed KA-induced increases in SCO frequency. D, LTG also normalized KA-induced decreases SCO amplitude. Each data point represents at least three replicates and the experiments were repeated twice in independent cultures with similar results. (**, $p<0.01$, KA vs Veh; $^{\#\#}$, $p<0.01$, LTG+KA vs 4-AP).

Figure 9|Lamotrigine normalized pilocarpine (10μM)-induced Ca^{2+} response in 9 DIV HN cultures. A, Representative traces showing the actions of lamotrigine (LTG) on pilocarpine-induced Ca^{2+} dynamics. B, Expanded traces showing LTG actions on pilocarpine-induced Ca^{2+} responses. C, LTG reversed the pilocarpine-induced prolongation of SCO lifetime. Each data point represents at least three replicates and the experiments were repeated twice in independent cultures with similar results. (**, $p<0.01$, pilocarpine vs Veh; $^{\#\#}$, $p<0.01$, pilocarpine+ LTG vs pilocarpine)

Figure 1

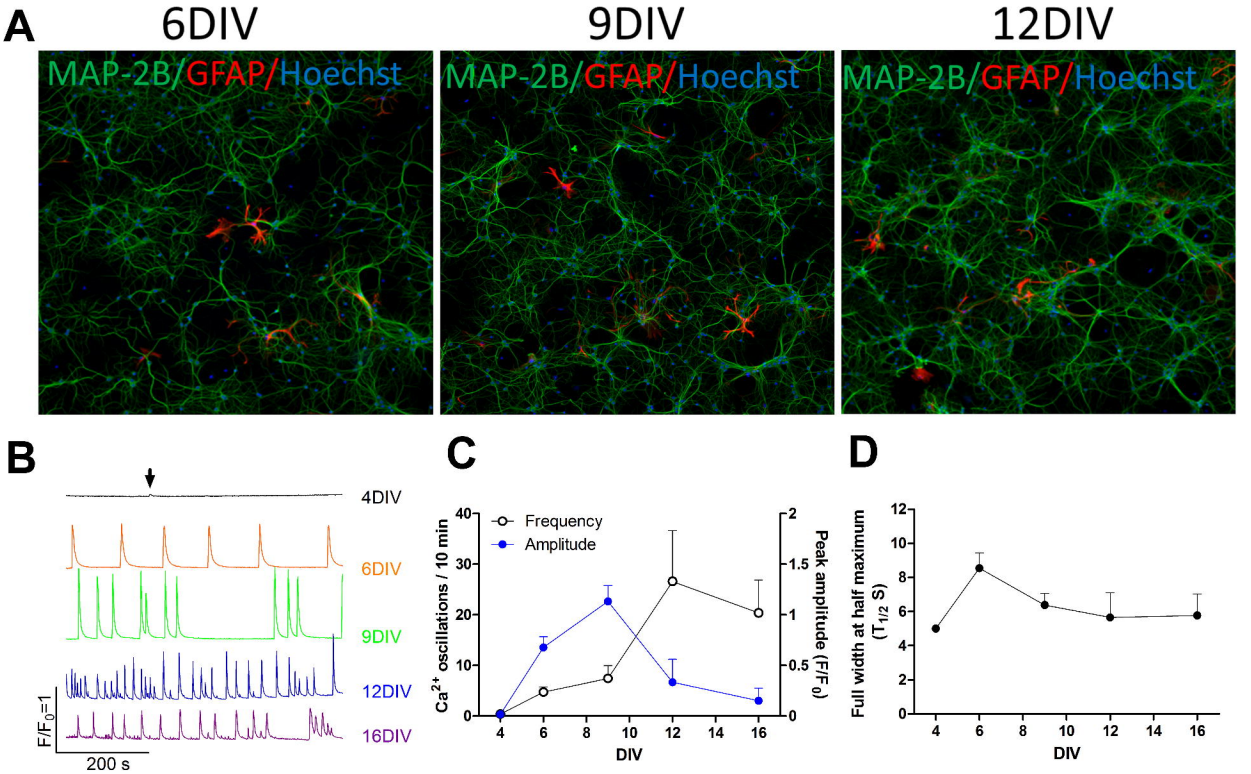
A
6DIV
9DIV
12DIV
MAP-2B/GFAP/Hoechst
MAP-2B/GFAP/Hoechst
MAP-2B/GFAP/Hoechst
B
4DIV
6DIV
9DIV
12DIV
16DIV
F/F0=1
200 s
C
Frequency
Amplitude
Ca2+ oscillations / 10 min
Peak amplitude (F/F0)
DIV
D
Full width at half maximum (T1/2 S)
DIV

Figure 2

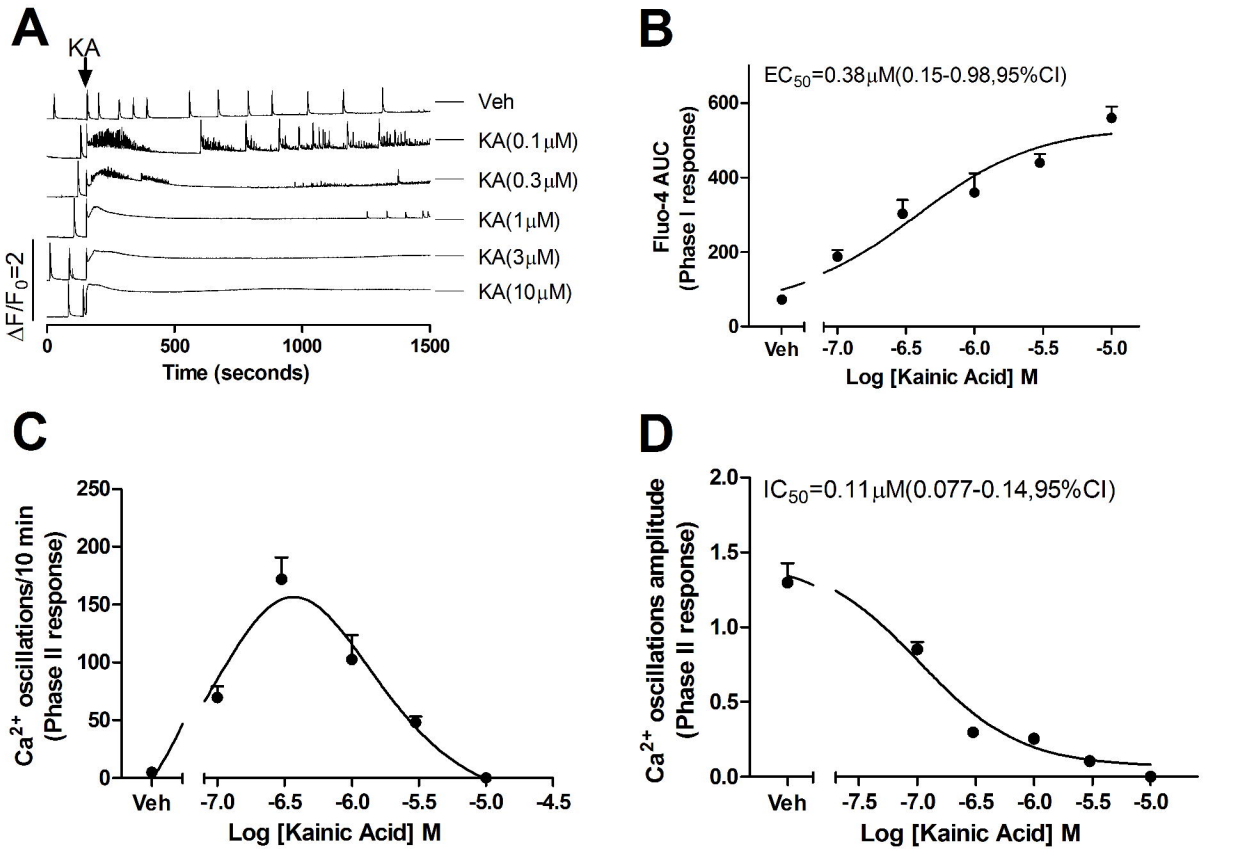
A
KA
Veh
KA(0.1μM)
KA(0.3μM)
KA(1μM)
KA(3μM)
KA(10μM)
ΔF/F0=2
0
500
1000
1500
Time (seconds)
B
EC50=0.38μM(0.15-0.98,95%CI)
Fluo-4 AUC
(Phase I response)
600
400
200
0
Veh
-7.0
-6.5
-6.0
-5.5
-5.0
Log [Kainic Acid] M
C
Ca2+ oscillations/10 min
(Phase II response)
250
200
150
100
50
0
Veh
-7.0
-6.5
-6.0
-5.5
-5.0
-4.5
Log [Kainic Acid] M
D
IC50=0.11μM(0.077-0.14,95%CI)
Ca2+ oscillations amplitude
(Phase II response)
2.0
1.5
1.0
0.5
0.0
Veh
-7.5
-7.0
-6.5
-6.0
-5.5
-5.0
Log [Kainic Acid] M

Figure 3

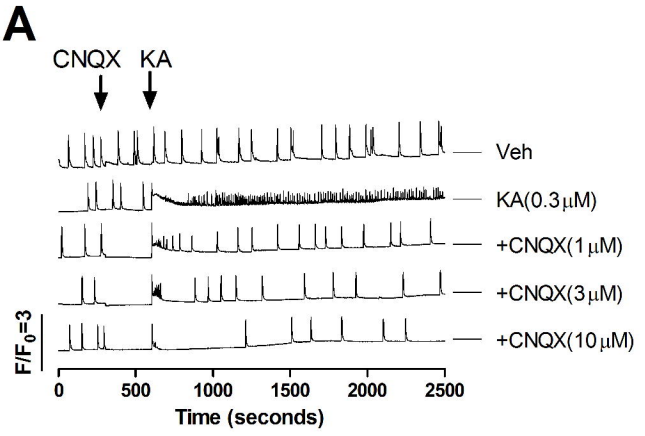
A
CNQX
KA
Veh
KA(0.3μM)
+CNQX(1μM)
+CNQX(3μM)
+CNQX(10μM)
F/F0=3
0
500
1000
1500
2000
2500
Time (seconds)

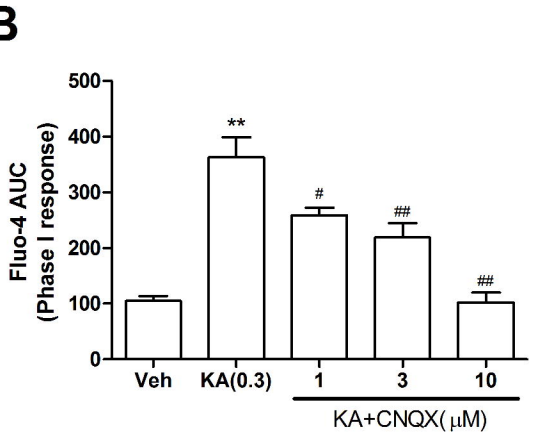
B
Fluo-4 AUC
(Phase I response)
500
400
300
200
100
0
**
#
##
##
Veh
KA(0.3)
1
3
10
KA+CNQX(μM)

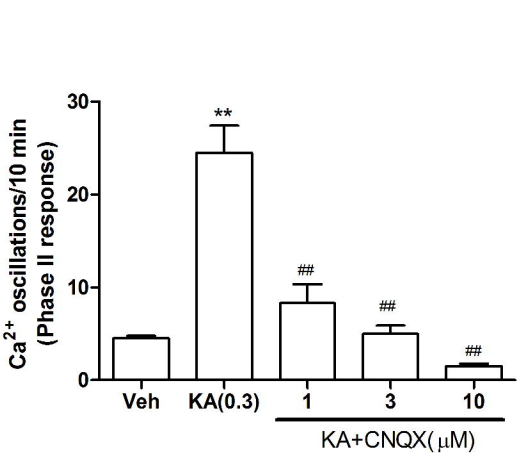
C
Ca2+ oscillations/10 min
(Phase II response)
30
20
10
0
**
##
##
##
Veh
KA(0.3)
1
3
10
KA+CNQX(μM)

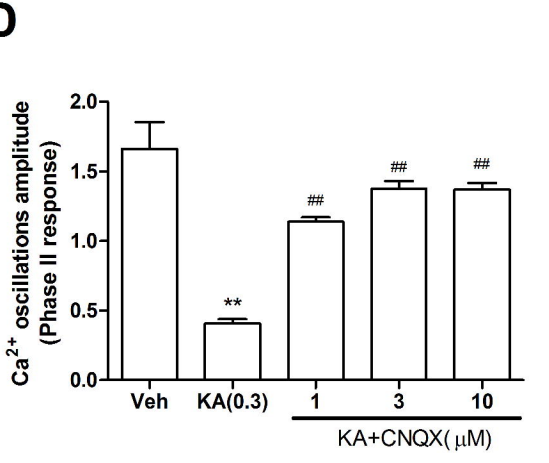
D
Ca2+ oscillations amplitude
(Phase II response)
2.0
1.5
1.0
0.5
0.0
**
##
##
##
Veh
KA(0.3)
1
3
10
KA+CNQX(μM)

Figure 4

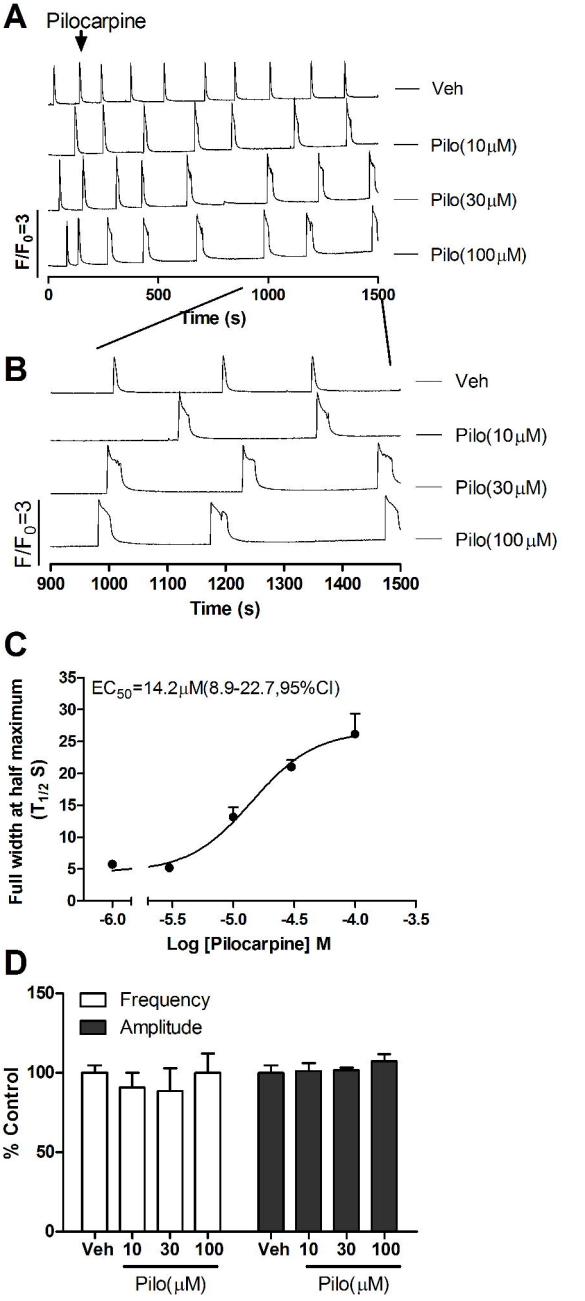
A
Pilocarpine
Veh
Pilo(10μM)
Pilo(30μM)
Pilo(100μM)
F/F0=3
0
500
1000
1500
Time (s)
B
Veh
Pilo(10μM)
Pilo(30μM)
Pilo(100μM)
F/F0=3
900
1000
1100
1200
1300
1400
1500
Time (s)
C
EC50=14.2μM(8.9-22.7,95%CI)
Full width at half maximum (T1/2 S)
35
30
25
20
15
10
5
0
-6.0
-5.5
-5.0
-4.5
-4.0
-3.5
Log [Pilocarpine] M
D
Frequency
Amplitude
% Control
150
100
50
0
Veh
10
30
100
Pilo(μM)
Veh
10
30
100
Pilo(μM)

Figure 5

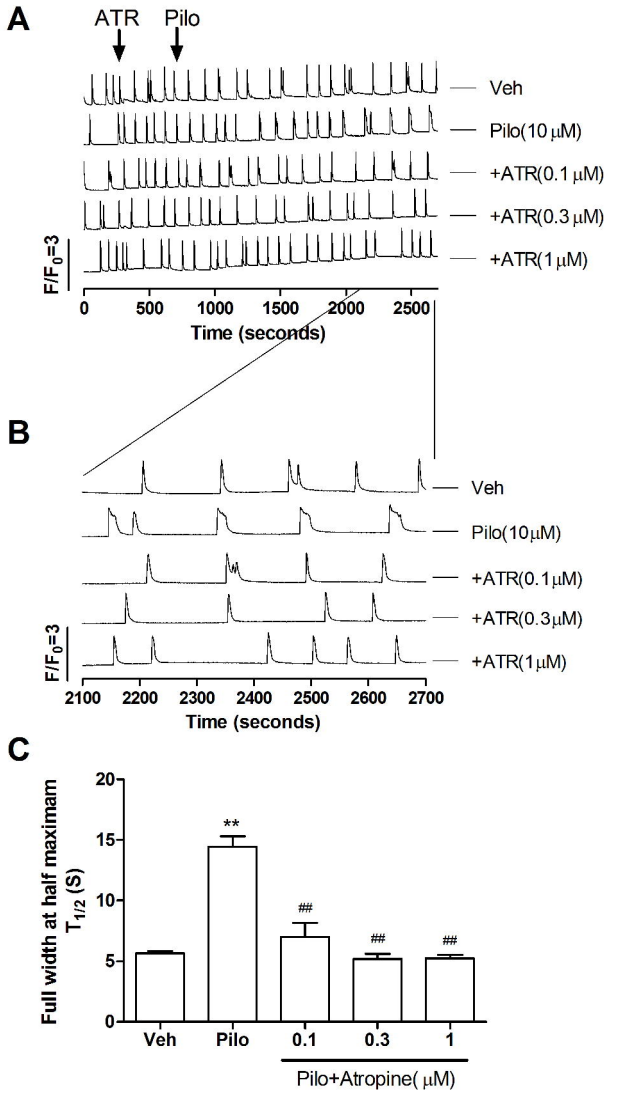
A
ATR
Pilo
Veh
Pilo(10 μM)
+ATR(0.1 μM)
+ATR(0.3 μM)
+ATR(1 μM)
F/F0=3
0
500
1000
1500
2000
2500
Time (seconds)
B
Veh
Pilo(10μM)
+ATR(0.1μM)
+ATR(0.3μM)
+ATR(1μM)
F/F0=3
2100
2200
2300
2400
2500
2600
2700
Time (seconds)
C
Full width at half maximam
T1/2 (S)
20
15
10
5
0
**
##
##
##
Veh
Pilo
0.1
0.3
1
Pilo+Atropine(μM)

Figure 6

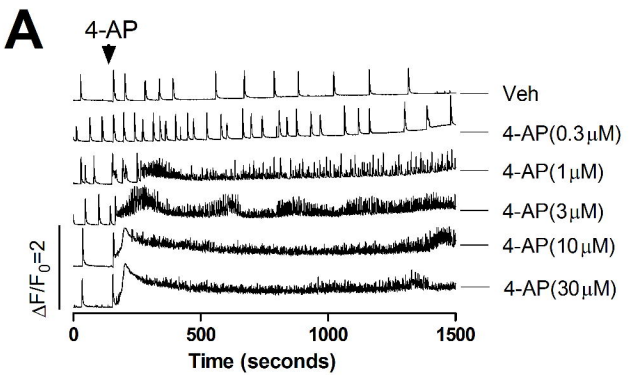
A
4-AP
Veh
4-AP(0.3μM)
4-AP(1μM)
4-AP(3μM)
4-AP(10μM)
4-AP(30μM)
ΔF/F0=2
0
500
1000
1500
Time (seconds)

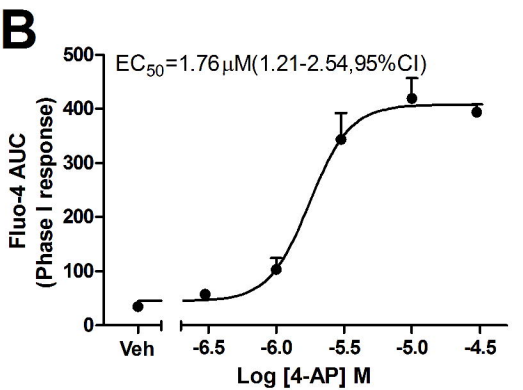
B
EC50=1.76μM(1.21-2.54,95%CI)
Fluo-4 AUC
(Phase I response)
500
400
300
200
100
0
Veh
-6.5
-6.0
-5.5
-5.0
-4.5
Log [4-AP] M

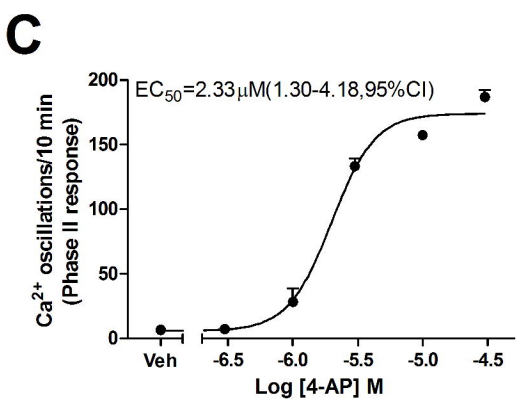
C
EC50=2.33μM(1.30-4.18,95%CI)
Ca2+ oscillations/10 min
(Phase II response)
200
150
100
50
0
Veh
-6.5
-6.0
-5.5
-5.0
-4.5
Log [4-AP] M

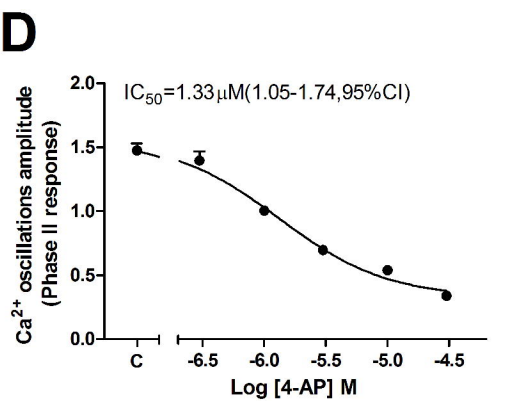
D
IC50=1.33μM(1.05-1.74,95%CI)
Ca2+ oscillations amplitude
(Phase II response)
2.0
1.5
1.0
0.5
0.0
C
-6.5
-6.0
-5.5
-5.0
-4.5
Log [4-AP] M

Figure 7

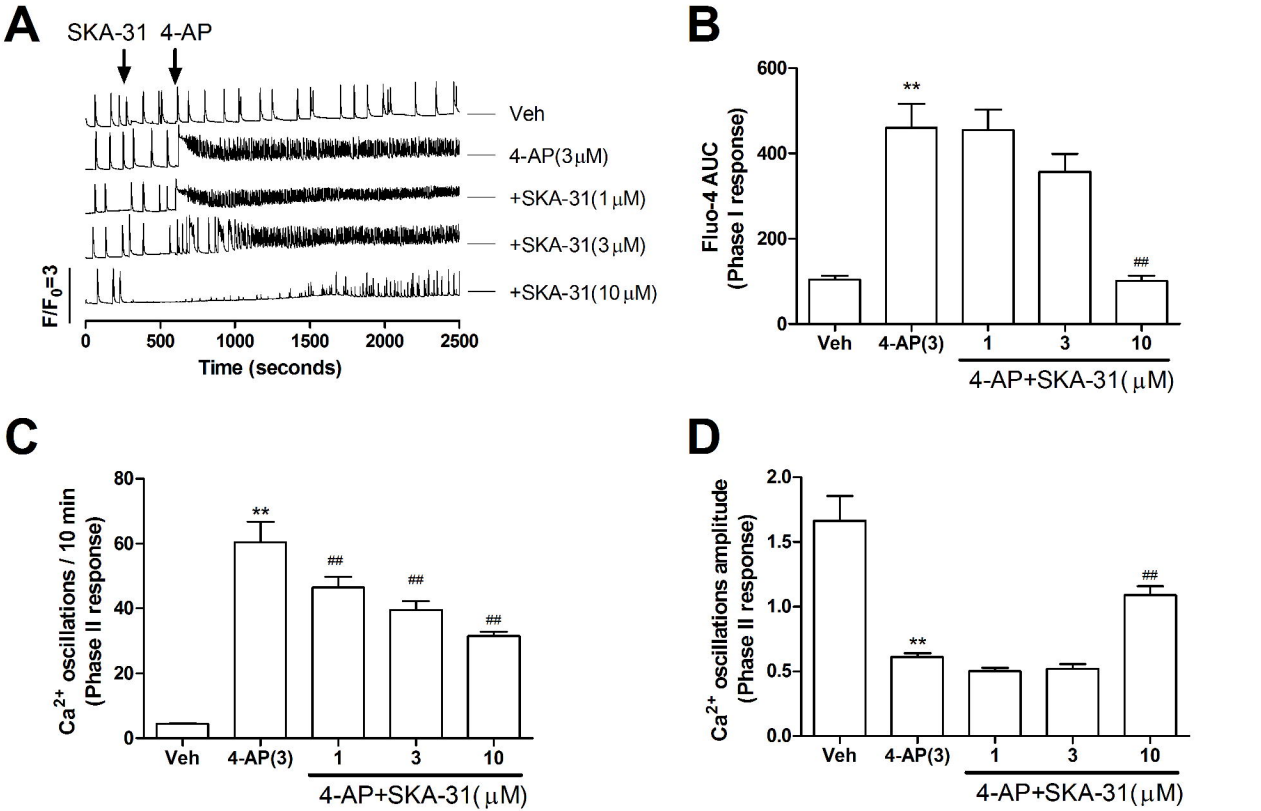
A
SKA-31
4-AP
Veh
4-AP(3μM)
+SKA-31(1μM)
+SKA-31(3μM)
+SKA-31(10μM)
F/F0=3
0
500
1000
1500
2000
2500
Time (seconds)
B
Fluo-4 AUC
(Phase I response)
600
400
200
0
**
##
Veh
4-AP(3)
1
3
10
4-AP+SKA-31(μM)
C
Ca2+ oscillations / 10 min
(Phase II response)
80
60
40
20
0
**
##
##
##
Veh
4-AP(3)
1
3
10
4-AP+SKA-31(μM)
D
Ca2+ oscillations amplitude
(Phase II response)
2.0
1.5
1.0
0.5
0.0
**
##
Veh
4-AP(3)
1
3
10
4-AP+SKA-31(μM)

Figure 8

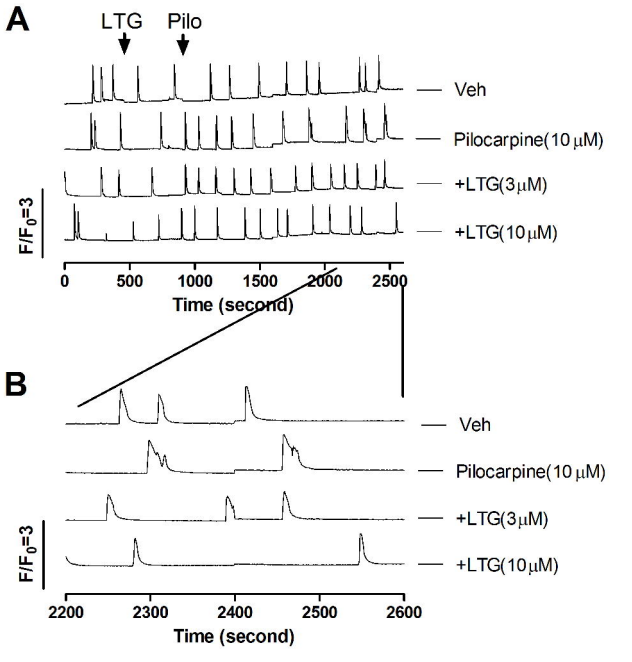
A
LTG
Pilo
Veh
Pilocarpine(10 μM)
+LTG(3μM)
+LTG(10μM)
F/F0=3
0
500
1000
1500
2000
2500
Time (second)
B
Veh
Pilocarpine(10 μM)
+LTG(3μM)
+LTG(10μM)
F/F0=3
2200
2300
2400
2500
2600
Time (second)

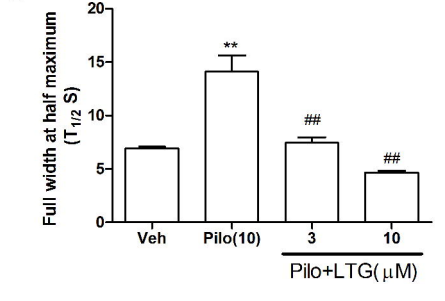
C
Full width at half maximum (T1/2 S)
20
15
10
5
0
**
##
##
Veh
Pilo(10)
3
10
Pilo+LTG(μM)

Figure 9

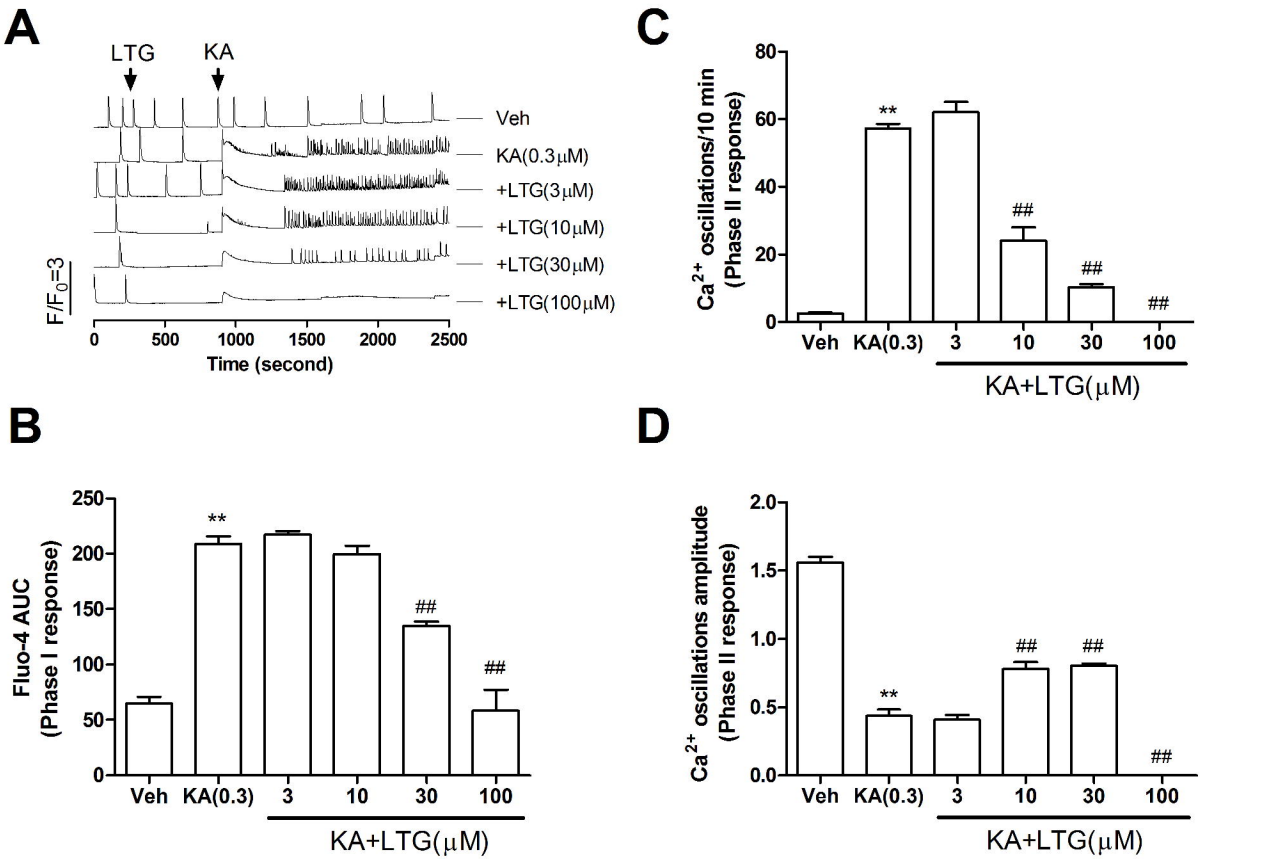
A
LTG
KA
Veh
KA(0.3μM)
+LTG(3μM)
+LTG(10μM)
+LTG(30μM)
+LTG(100μM)
F/F0=3
0
500
1000
1500
2000
2500
Time (second)
C
Ca2+ oscillations/10 min
(Phase II response)
80
60
40
20
0
**
##
##
##
Veh
KA(0.3)
3
10
30
100
KA+LTG(μM)
B
Fluo-4 AUC
(Phase I response)
250
200
150
100
50
0
**
##
##
Veh
KA(0.3)
3
10
30
100
KA+LTG(μM)
D
Ca2+ oscillations amplitude
(Phase II response)
2.0
1.5
1.0
0.5
0.0
**
##
##
##
Veh
KA(0.3)
3
10
30
100
KA+LTG(μM)